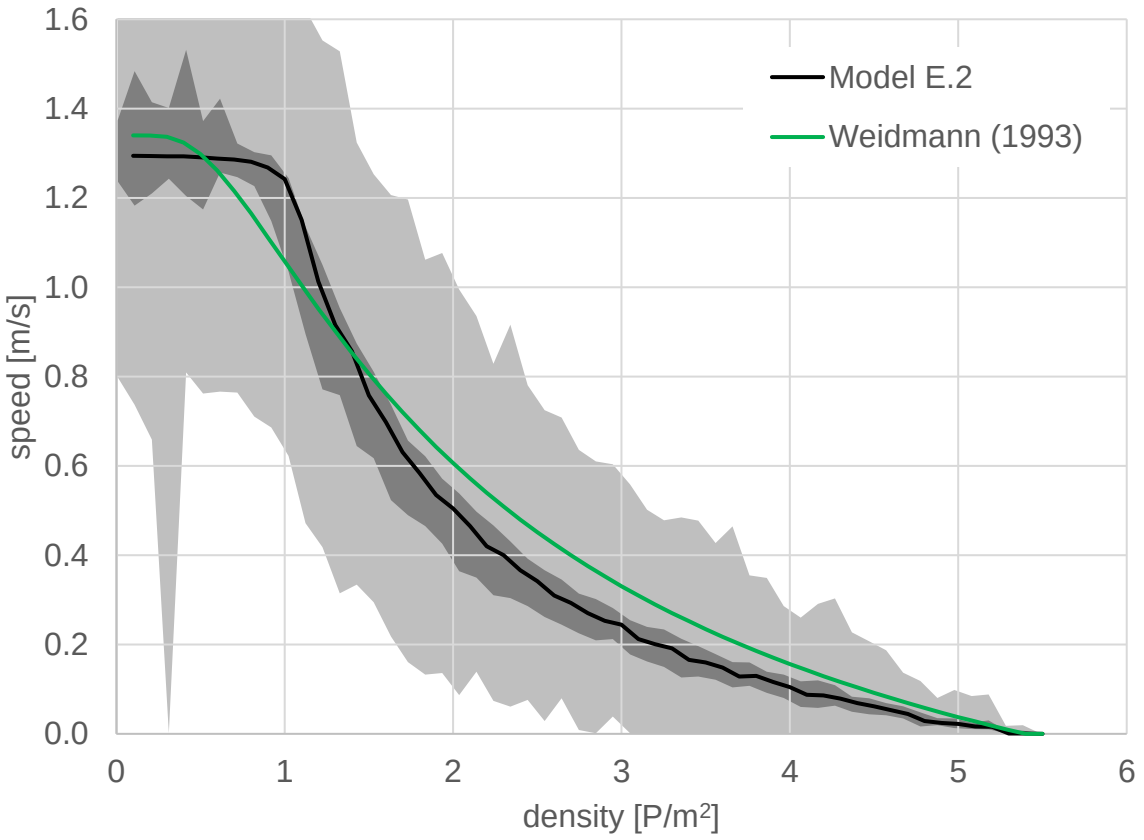

Creating a generic model of the pedestrian fundamental diagram

Ernst Bosina, ETH Zürich
Ulrich Weidmann, ETH Zürich

Conference Paper STRC 2018

STRC | 18th Swiss Transport Research Conference
Monte Verità / Ascona, May 16-18, 2018

Creating a generic model of the pedestrian fundamental diagram

Ernst Bosina
ETH Zürich
Zürich
T: +41 44 633 72 36
E: ebosina@ethz.ch

Ulrich Weidmann
ETH Zürich
Zürich
T: +41 44 632 05 91
E: weidmann@sl.ethz.ch

May 2018

Abstract

Pedestrian characteristics, such as their free-flow walking speed, vary considerably between individuals and for different situations. This is also reflected in the pedestrian fundamental diagram, where considerable differences are visible. As the fundamental diagram serves as a tool for the design of pedestrian facilities, accurate values are needed for an efficient and functional design. Nevertheless, up to now no method exist, which can be used to determine a suitable fundamental diagram for a specific facility without the need for measurements in similar situations.

This paper presents a generic approach to describe the pedestrian fundamental diagram. By combining literature data about aspects of pedestrian movement and interactions while walking, a fundamental diagram model is created, which is as close as possible to the real human walking behavior. By adapting the pedestrian properties, it is possible to study the effect of the situation-specific setting on the fundamental diagram. The resulting fundamental diagram model can then be used to obtain fundamental diagrams adapted to a specific situation and thus enhance the design of pedestrian facilities.

Keywords

Pedestrian; Fundamental diagram; Generic model

1. Introduction

The pedestrian fundamental diagram describes the average relation between flow, speed and density in steady state conditions (Bosina and Weidmann, 2016). It is one of the main tools for the analytical design of pedestrian facilities, but it is also an important concept used to describe the properties of a pedestrian flow. Still, fundamental diagrams created from experimental data and mathematical models show considerable differences. This can partly be explained by different measurement methods, but is also due to the pedestrian and facility characteristics, which have a strong influence on the shape of the fundamental diagram. However, up until now no model exist, which can include these differences and hence produce a suitable fundamental diagram for each specific situation. Therefore, today a general fundamental diagram is used, if no specific measurements are available. This will lead to poorly designed pedestrian facilities, as the real walking behavior might be considerably different than the assumed average.

The goal of this work is to set up a generic fundamental model, which can be used to determine the influence of different pedestrian compositions on the fundamental diagram. Hence, for each situation, a specific fundamental diagram can be calculated. The model will be based on a throughout literature review about human walking and the interaction of pedestrians while walking, which is partly published in Bosina and Weidmann (2016) and Bosina and Weidmann (2017). This paper now focuses on the creation of the fundamental diagram model for a unidirectional flow. Thus, the literature review on the human walking principles is not part of this paper, but was done separately.

Several microscopic model approaches exist in literature for the simulation of pedestrian flows (see for example Duives et al. (2013) or Reda (2017)). Among these, most models use analogies or otherwise do not aim at modelling the walking behavior, as it shall be done here in the fundamental diagram model. For example, the widely used social force model (Helbing and Molnár, 1995) uses the analogy of forces to calculate the accelerations while walking and thus the walking behavior. But other models, such as the Follow-The-Leader model (Degond et al., 2015), the optimal step model (Seitz and Köster, 2012), visual based models (Kang and Han, 2017; Moussaïd et al., 2011) or energy based models (Guy et al., 2010) are aiming at directly describing at least parts of the walking principles. These models will therefore be used as a starting point for the model setup.

2. Modelling approach

2.1 Modelling steps

Table 1: List of models created and their main properties

Model	Modelled space	Update	Decision	Other aspects added
Model A	Single lane	every time step / deterministic	instantaneous	
Model B	Single lane	global walking step duration	one step ahead	
Model C	Single lane	individual step length	decision time before step change	acceleration limitation, random noise
Model D	Single lane	individual step length	prediction for time of step change	
Model E	parallel lanes	individual step length	prediction for time of step change	switching lanes

As the interaction between pedestrians is complex, the fundamental diagram model will also be developed starting with simplifications and gradually increasing the complexity. The complexity of modelling the pedestrian flow is mainly based on two aspects. First, the flow itself can be complex, which will be included in the model creation by first starting with a single lane and then adding additional lanes in a later model to allow overtaking. For the final step, a fully unidirectional model where pedestrian move in a 2D space, no satisfying model results were obtained, therefore this model is excluded from this paper. The second aspect is the variation of the pedestrian properties. For the least complex situation, these properties can be set to be equal for all pedestrians, which makes it easier to calculate the fundamental diagram, at least for a simple case. Again, this assumption will be dropped to also study the influence of variations in the pedestrian composition. In Table 1, the list of models created for this work and their main characteristics are shown, which provides an overview about the main modelling steps.

Only for the first modelling step, Model A of the lane-based models, the steady state condition can be obtained directly using the formula without the need of iterations. All other models are based on a time-step approach. For each global density, a set of pedestrians is generated and initial speeds and positions are determined. Then, the simulation is done for a defined number of time-steps, until steady state conditions are expected.

2.2 Model layout

The simulation area is modelled as infinite loop, where pedestrians reaching the end of the track start again at the beginning of the track. Also, the lateral limits of the area are connected, hence people leaving the area on one side will enter on the other side. Thus, the size of the simulation area is only relevant for the modelling, no wall effects occur in the model.

Figure 1: Example of the fundamental diagram plot from the model result. Black curve: average speed; dark grey: range of individual walking speeds over a longer time period; light grey: instantaneous walking speeds; green: fundamental diagram from Weidmann (1993).

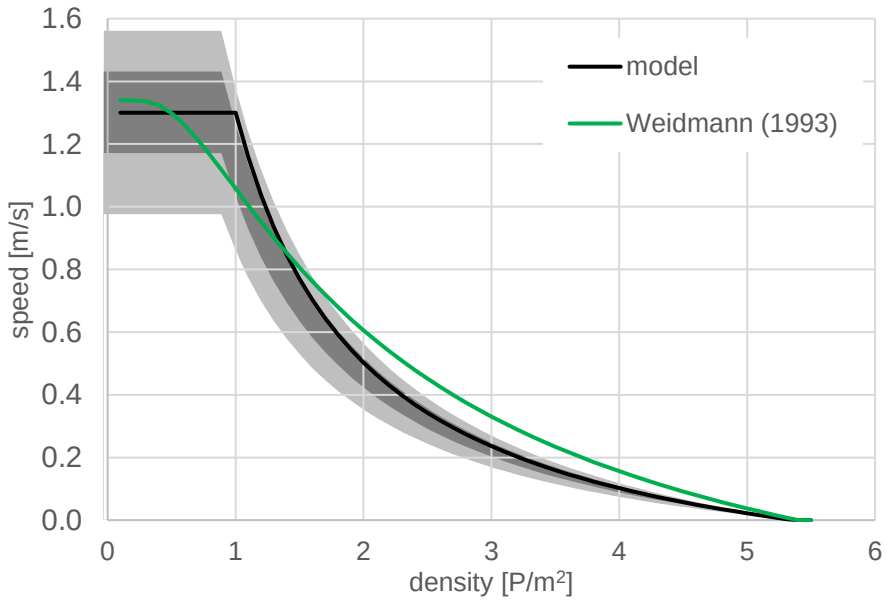

The model results are usually presented as shown in the example in Figure 1. Here, not only the average walking speed is shown, as it is done in the regular fundamental diagrams, but also the range of walking speed measurements. The dark grey area indicates the speed distribution computed using the average individual walking speed, hence one average value per person. The light grey area shows the distribution of the instantaneous walking speeds. For comparison, the fundamental diagram from Weidmann (1993) is also added to the figure.

2.3 Model parameter

For the basic model variables, literature data is available which allows to estimate the range of their values (Table 2). For the deceleration time it was assumed that the deceleration needs one to two steps, independent on the walking speed and that these steps are done at the full walking

speed chosen. For the pedestrian composition parameters either a minimum, maximum, average or uniform distribution is used for the model setup. For the minimum and maximum variable compositions extreme values are used, so that for the minimum composition the lowest speed at a certain density and for the maximum composition the highest speed is obtained. The uniform and average composition are both based on the range of values presented. In addition to the pedestrian properties, several other simulation parameters were introduced. These are shown in Table 3 and will be further described when they are introduced into the model.

Table 2: Range of values for the pedestrian characteristics used for modelling the fundamental diagram. The minimum and maximum values in the range of values are set, so that the minimum will result in a minimum walking speed for a given density and the maximum for a maximum speed.

Variable	Minimum	Maximum	Source
Desired walking speed v_d [m/s]	1.00	1.60	Bosina and Weidmann (2017)
Body width w_B [m]	0.49	0.33	DIN (2013), Pheasant (2006)
Sway width w_S [m]	0.06	0.04	Murray et al. (1964), Simoneau (2010)
Body depth d_B [m]	0.29	0.17	DIN (2013), Still (2000).
Intimate distance d_I [m]	0.20	0.15	Hall (1966)
Reaction time t_r [s]	0.80	0.40	Degond et al. (2015), Ma et al. (2010), Moussaïd et al. (2009)
Deceleration time t_d [s]	1.02	0.49	Hediyeh et al. (2015)

Table 3: Simulation parameter

Parameter	Default value		Introduced in
Number of pedestrians	1’000		Model A
Simulation time interval	0.1	s	Model A
Simulation duration	10’000	s	Model A
Number of time steps used for speed calculation	1’000		Model A
Random noise	10	%	Model C
Step formula	Cavagna		Model C
Maximum acceleration	0.6	m/s^2	Model C
Reaction delay	0.2 – 0.4	s	Model C
Maximum reaction time	1	s	Model C
Minimum walking speed	0	m/s	Model C
Number of lanes	10		Model E
Backward distance for lane change	3	m	Model E
Initial time steps with no lane change	100		Model E
Maximum reaction headway	4	m	Model E

3. Lane-based models

3.1 Model description

For the lane-based models, walking is simulated as a one-directional movement, where pedestrians walk in predefined lanes without interaction between lanes. Thus, no side movement exists. In this case, it can be assumed that each pedestrian is only reacting to the pedestrian directly in front. In addition, the only reaction possibility is the change of walking speed, as no sideward evasion is possible. To obtain a two-dimensional fundamental diagram for this situation, a lane width has to be defined, which is assumed to equal the average body and sway width.

As the pedestrians cannot overtake each other, faster pedestrians have to reduce their walking speed when approaching a slower pedestrian in front. As the fundamental diagram definition used requires steady state conditions, this will only be reached if all pedestrians show the same (slowest) walking speed. Therefore, the linear model cannot be used to determine the influence of different desired walking speeds but an average walking speed has to be used for the model to be useful. At higher densities, overtaking is expected to be less relevant and the all pedestrians will walk at speeds lower than desired. In this case, the missing possibility of overtaking will not influence strongly the results.

3.2 Model layout

Table 4: Speed change and time of speed change procedure for the different lane based models.

Model	Speed change	Time of speed decision
Model A	every time step / deterministic	instantaneous
Model B	global walking step duration	one step ahead
Model C	individual step length	certain time before step change
Model D	individual step length	prediction for time of step change

In chapter 3.3 to 3.6, four models (Model A to Model D) will be presented. The models are based on its predecessors and will step by step add features which will improve the consistency of the model with the human walking principles. One important aspect addressed in the model improvements is the time and amount of possible speed changes and the time, when the next speed is decided (Table 4). In Model A, every time step a speed update is possible, which is

based on the information currently available. For the last model (Model D), a speed change is only possible at the end of a step. In addition, this change is done on a prediction based on the situation a certain time interval before the end of the step.

Each model can be run using different simulation parameter values. In Table 5, the values for the simulations presented in the figures of this paper are shown. As overtaking is not possible in the lane-based models, the uniform distribution is computed without a free-flow speed distribution. Otherwise, as the model runs until steady state conditions are reached, everyone would align behind the slowest pedestrian, who will determine the average walking speed. Therefore, the average walking speed is used for all pedestrians for the uniform distribution. Only Model D.5 uses a speed distribution to compare the effect to Model D.2. For all parameter values not shown, the default values from Table 3 are used.

Table 5: Parameter values used in this chapter.

Model	Interval [s]	Distribution	Random noise	Step formula	Max. acceler-ation [m/s^2]	Reaction delay [s]	Figure
A.1-3	-	min/max/av	-	-	-	-	Figure 3
B.1	0.45	uniform	-	-	-	-	Figure 5 Figure 7
B.2	0.50	uniform.	-	-	-	-	Figure 6 Figure 8
C.1	0.10	uniform.	0%	Cavagna	2.0	0.2	Figure 10
C.2	0.10	uniform.	0%	Cavagna	2.0	0.2 - 0.4	Figure 11
C.3	0.10	uniform.	0%	Jelic	2.0	0.2 - 0.4	Figure 12
C.4	0.10	uniform.	0%	Cavagna	0.6	0.2 - 0.4	Figure 13
C.5	0.10	uniform.	0%	Cavagna	0.3	0.2 - 0.4	Figure 14
C.6	0.10	uniform	10%	Cavagna	0.6	0.2 - 0.4	Figure 15
D.1	0.10	average	10%	Cavagna	0.6	0.2 - 0.4	Figure 18
D.2	0.10	uniform	10%	Cavagna	0.6	0.2 - 0.4	Figure 17 Figure 20
D.3	0.10	maximum	10%	Cavagna	0.6	0.2 - 0.4	Figure 18 Figure 19
D.4	0.10	minimum	10%	Cavagna	0.6	0.2 - 0.4	Figure 18
D.5	0.10	uniform	10%	Cavagna	0.6	0.2 - 0.4	Figure 20

3.3 Model A: basic lane model

3.3.1 Uniform pedestrians

The simplest form, where a fundamental diagram can be calculated, is a single lane of pedestrians showing the same properties. For this model, it is assumed that constant conditions exist. Hence, delays in reaction and other factors which might produce variations at stable conditions do not occur. Therefore, at constant densities, no speed differences will occur. Thus, the fundamental diagram solely depends on the speed, a pedestrian keeps at a certain distance to the pedestrian in front, and the width of each lane.

The speed-distance relationship can be further divided into speed independent components and speed dependent ones. Speed independent components and thus constant are the body depth and the intimate distance, which is considered to be also respected while standing at the closest comfortable distance. The reaction distance and the deceleration distance are speed-dependent. The lane width can be calculated using the body width and the gait cycle sway.

At low densities, the desired walking speed is determining the chosen walking speed, at a certain density, the walking speed can be set to zero, as the limited space does not allow further movement. In between, the walking speed depends on the pedestrian density. For the single-file movement, for each speed, a headway distance needed can be calculated. This headway distance consists of constant parts, the body depth d_B and the intimate distance d_I, and of speed dependent parts, namely the reaction and deceleration distance (Figure 2).

Figure 2: Headway distance in single-file movement

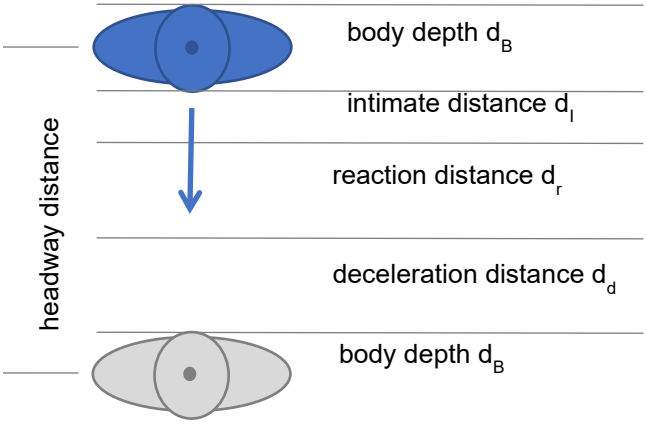

The pedestrian density can then be obtained using the calculated headway distance and the lane width. The lane width itself can be calculated using the body width w_B and the gait cycle sway w_S:

$$w_L = w_B + w_S \quad (1)$$

w_L lane width [m]
w_B body width [m]
w_S sway width [m]

In a first approach, the headway is calculated using the formula:

$$h = \frac{1}{D * w_L} \quad (2)$$

h headway distance [m]
D pedestrian density [P/m2]
w_L lane width [m]

When summarizing the influences, the following equation can be derived, describing the density dependent walking speed:

$$v = v_d \quad \textit{for} \quad D > \frac{1}{\left((d_B + d_I) + (t_r + t_d) * v_d\right) * w_L} \quad (3)$$

$$v = \frac{h - (d_B + d_I)}{t_r + t_d} \quad \textit{for} \quad D \geq \frac{1}{(d_B + d_I) * w_L} \quad (4)$$

v chosen walking speed [m/s]
v_d desired walking speed [m/s]
D pedestrian density [P/m2]
d_B body depth [m]
d_I intimate distance [m]
t_r reaction time [s]
t_d deceleration time [s]
w_L lane width [m]

The range of the fundamental diagrams calculated using the presented formula and the range of variables can be seen in Figure 3. The fundamental diagram for walkways presented by Weidmann (1993) is well within this range. Still, as the model assumes uniform pedestrian characteristics, it is expected that a general unidirectional fundamental diagram shows lower walking speeds for the same densities, as pedestrians have to adapt themselves to the pedestrian in front.

Figure 3: Model A.1-3: range of calculated fundamental diagrams compared with the fundamental diagram from Weidmann (1993) and the speed-density data from Bosina and Weidmann (2017).

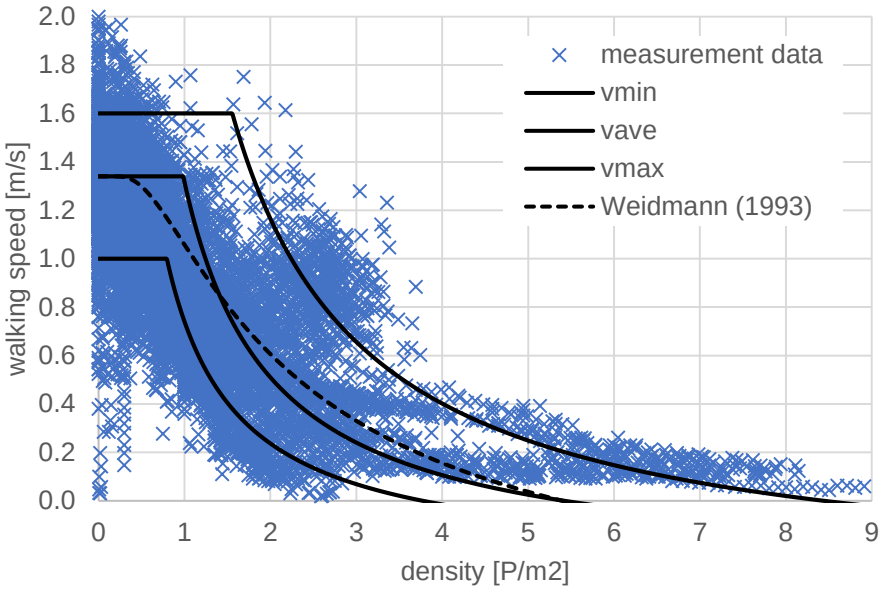

3.3.2 Lane movement with single property variation

When walking in line, pedestrian cannot overtake each other. Thus, pedestrians showing a higher desired walking speed have to slow down and adapt to the pedestrian in front, resulting in a walking speed corresponding to the slowest pedestrian in front. In addition, the pedestrian characteristics, such as body depth or reaction time might vary between pedestrians. This results in different headways required to keep a certain speed. As the speed shall be the same for all pedestrians, different headways will be established, depending on the pedestrian characteristics.

In this model extension, each property is varied between the maximum and minimum values obtained from literature and presented in Table 2. This allows to discuss the individual effects on the fundamental diagram.

When the model is extended to allow a distribution in the body depth and/or the intimate distance, it can be seen that only the average values influence the fundamental diagram, the distribution of these values has no influence. In the current model, for a given density, the walking speed is equal for all pedestrians, as overtaking is impossible and no fluctuations are considered. Hence it is assumed that the headway for each pedestrian is optimized, so that all pedestrians have the minimum headway for the highest speed possible. Therefore, people

showing larger body depth or intimate distance will have higher headways than other pedestrians, resulting in the same speed for everyone. In the fundamental diagram model, the body depth and intimate distance can thus be substituted by their average values to calculate the speed for a given density.

As overtaking is impossible in the lane movement situation considered, the slowest walking speed determines the walking speed of all pedestrians in steady state conditions. Thus, also the slowest desired walking speed has to be considered when determining the fundamental diagram curve.

The width of each lane is determined using the body width and the sway width. In a first approach it can be expected that here the maximum total value is determining the lane width.

Similar to the body depth and the intimate distance, also for the reaction distance and the deceleration distance, only their average values are relevant. It can therefore be concluded that using these simple models, no variations are visible in the fundamental diagram. Hence, the fundamental diagram does neither show any stochastic variations nor changes with differences in the variation of the input parameters. Still, experiments described in literature indicate that also the variation has an influence on the resulting fundamental diagram (Cao et al., 2016; Zhang et al., 2016).

3.4 Model B: introducing step duration

3.4.1 Introduction

An additional aspect relevant for the pedestrian flow is the time delay. The reaction of pedestrians to visual perceptions is not immediately but shows a certain time delay. In the previous models, this was modelled assuming a reaction time corresponding to a certain distance kept to the person in front. In addition to this, also the acceleration and deceleration starts with a certain delay. To also include this in the model, Model B separates the action point, where the change in walking speed occurs, and the decision point, where the decision for the next walking speed is made (Figure 4).

Figure 4: Model B: Modelled point of decision and action for a single step.

Based on the literature findings, the influence of the reaction delay will be refined in the next model step. For this step, the model cannot further be exclusively based on deterministic formulas. Therefore, a model framework is established in python, simulating individual pedestrians. For each density considered, a simulation is done until quasi-steady state conditions are reached, which are represented in the fundamental diagram. This approach also allows to study the distribution of walking speeds present at a certain global density.

3.4.2 Step length delay

The simplest possibility to introduce the reaction delay is to assume a constant delay for all pedestrians. In a first step, this is done by using the distance between two pedestrians from the previous time step to calculate the current speed instead of assuming an instant reaction to the distance as it was done in the previous models. From literature, it can be concluded that in general, an acceleration or deceleration movement is always initiated at the same phase of the walking cycle. Thus, the walking speed can mainly be adapted once for each step. The update cycle of the model shall therefore correspond to the step duration.

Combining the assumption of a single speed update each step and a reaction delay, the situations some time (the reaction delay) before the next step is considered to determine the next speed. As the update of the walking speed is done in parallel for all pedestrians in this model, the situations one walking step ahead equals the situation at the decision time, as long as the reaction delay is equal or smaller than one step. As additional boundary condition it is assumed that the pedestrians are not compressible, hence their minimal distance corresponds to the body depth. Nevertheless, due to the reaction delay, the intimate distance can be violated in this model.

From literature, an average step frequency of 1.75 – 2.16 Hz can be found at free flow walking speed (Kramers-de Quervain et al., 2008). This corresponds to a duration of 0.46 – 0.57 s

between two consecutive step initiations. Calculating the fundamental diagram based on this model and an update interval corresponding to one step reveals two distinct situations. For intervals shorter than 0.47 s, a homogeneous flow can be observed (Figure 5). For longer time intervals, stop and go waves are produced (Figure 6). In single-file movement experiments, stop and go waves were also observed, but only at linear densities of more than about 1.7 P/m (Portz and Seyfried, 2011; Ziemer et al., 2016). Although this behavior is not expected at this global density, the simulation results indicate that the reaction delay influence the resulting flow and thus the fundamental diagram.

Figure 5: Model B.1: Space-time diagram for a density of 2 P/m^2 and a simulated time interval of 0.45 s.

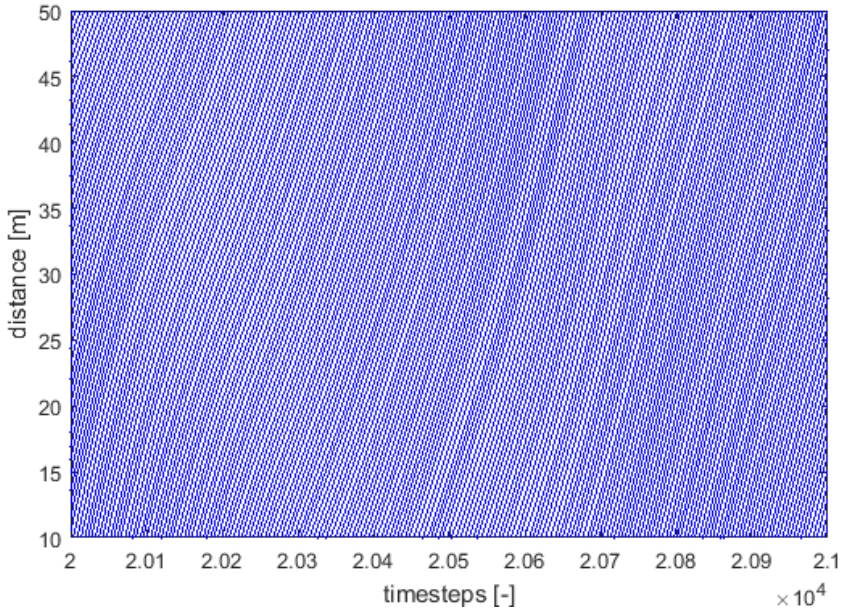

For short intervals, the obtained fundamental diagrams are the same as in the first model (Figure 7). The speed distribution shown does show some variations, which is assumed to be due to the fact that the pedestrians in the model do have a reaction delay which will lead to a variation in the instantaneous speeds. The average individual speeds are otherwise close to the global average speed.

For the time interval of 0.50 s, a slight change in the fundamental diagram is visible (Figure 8). The mean speed at densities between 1.0 and 1.5 P/m^2 is slightly lower, whereas at higher densities, the speed is higher. Also, a slightly higher maximum density was found.

Figure 6: Model B.2: Space-time diagram for a density of 2 P/m^2 and a simulated time interval of 0.5 s.

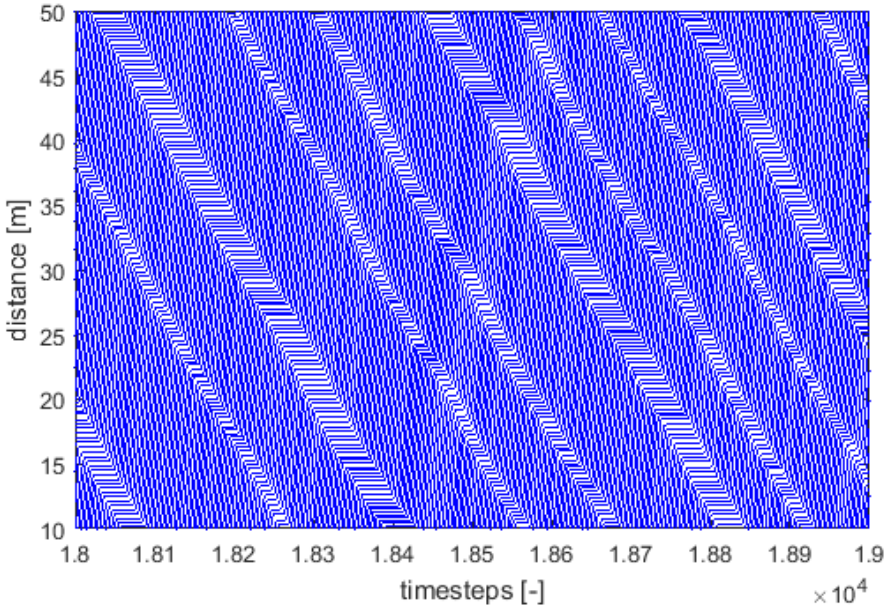

Whereas the distribution of average individual speeds is similar, the instantaneous speed shows a considerably stronger distribution. Starting with a density of about 1 P/m2, the instantaneous speed values vary between standing pedestrians and pedestrians walking at the free flow speed which is linked to the stop and go waves visible in the space-time diagram shown in Figure 6.

Figure 7: Model B.1: Speed-density diagram for a simulated time interval of 0.45 s.

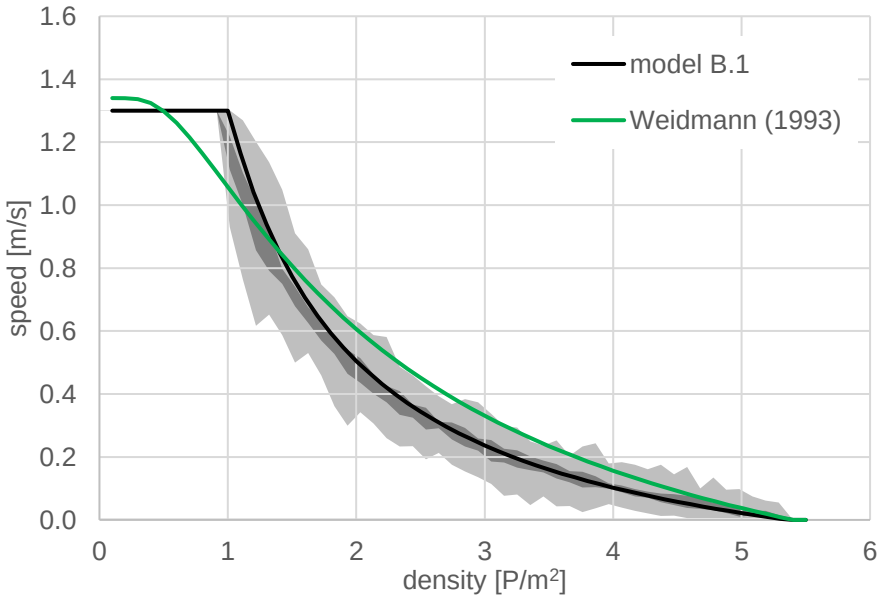

Figure 8: Model B.2: Fundamental diagram for a simulated time interval of 0.50 s.

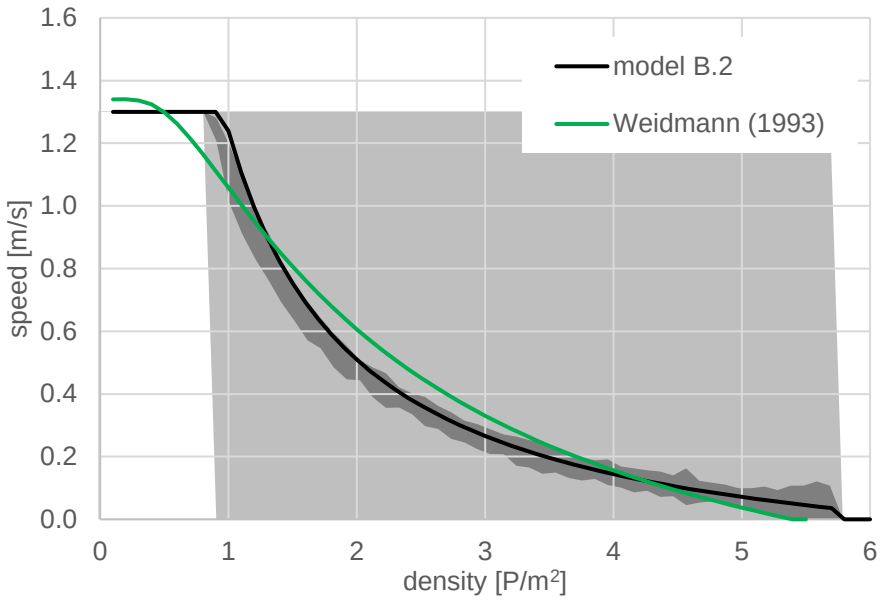

3.5 Model C: individual step length

3.5.1 Introduction

At higher walking speeds the step frequency increases, hence the walking cycle length decreases. Therefore, the constant time interval between speed adaptions as present in the previous model can be adapted to be dependent on the walking speed. Using the formula from Cavagna and Margaria (1966), the step duration can be calculated by:

$$D_s = \frac{0.362}{v} + 0.257 \quad (5)$$

D_s step duration [s]

v walking speed [m/s]

To include the fact that at low walking speeds only few data exists and speed changes are also possible within a gait cycle, a maximum step duration is set at 1.0 s.

In the previous model, the decision for step i+1 was done at the start of step i. Now the model is adapted, so that these two points are separated in time (Figure 9). This reflects the fact that a certain time is needed to obtain information, process it and initiate an action. Thus, the decision is made at a certain time interval before the action point, corresponding to the minimum time interval possible to update the movement. Until this time, a decision might be updated if new

information is available. Afterwards, no update, which can be applied at the action point, is possible. Still, also within a step, changes in speed and direction are possible, but as they involve higher effort and are not expected to take place regularly, these are omitted in this model.

Figure 9: Modelled point of decision and action for a single step.

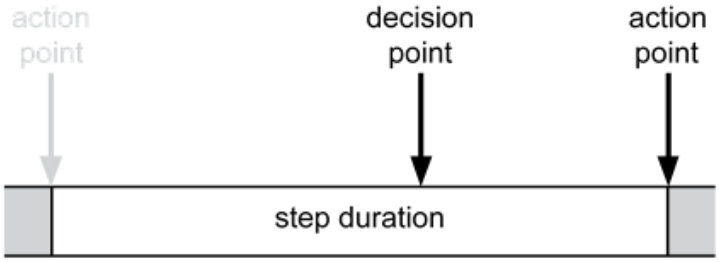

3.5.2 Reaction delay

As no information on the reaction time t_r between decision point and action point was found in literature, a value of 200 ms and a range between 200 and 400 ms is used as a first estimation. The results for both model runs do not show strong differences between these two reaction times (Figure 10 and Figure 11). At walking speeds higher than 2 P/m^2, the higher reaction times lead to slightly higher walking speeds and to higher maximum density (5.3 P/m^2 compared to 5.9 P/m^2).

Figure 10: Model C.1: Fundamental diagram for a reaction time tr = 0.2 s; Step duration calculated from Cavagna and Margaria (1966).

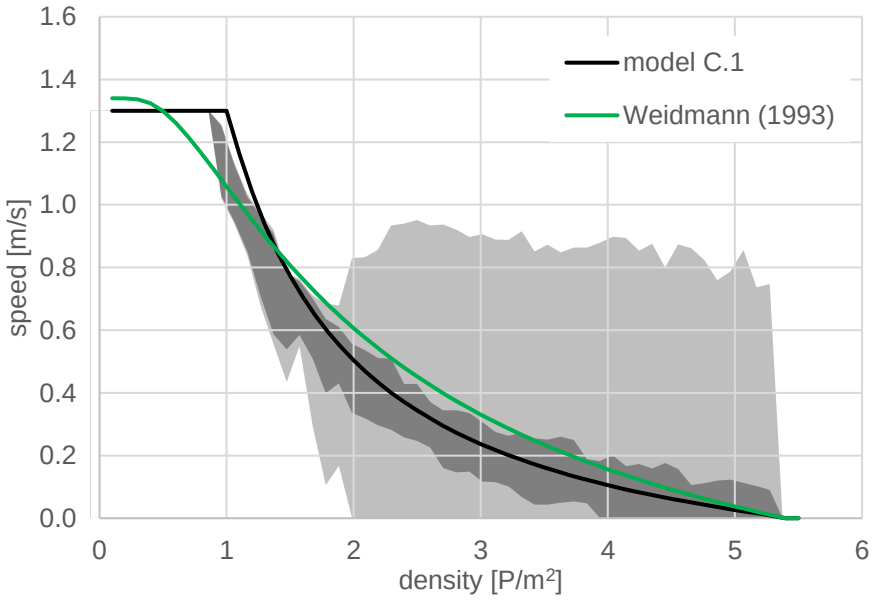

However, the biggest differences can be seen in the speed distribution. Whereas stop and go behavior is only visible for densities higher than 2 P/m^2 in Model C.1, it can be already seen at densities slightly higher than 1 P/m^2 in Model C.2, when keeping the free-flow speed is not possible any more. As discussed previously, this does not correspond to the expected pedestrian behavior. Still, the fundamental diagram curve is not considered to be influenced strongly by this model behavior. Therefore, no changes were made to the model parameters to determine, if this happens for all parameter combinations. As this is an intermediate model stage, the occurrence of stop and go waves will be discussed in a later model stage, if they are then still visible.

Figure 11: Model C.2: Fundamental diagram for a reaction time tr = 0.2 – 0.4 s; Step duration calculated from Cavagna and Margaria (1966).

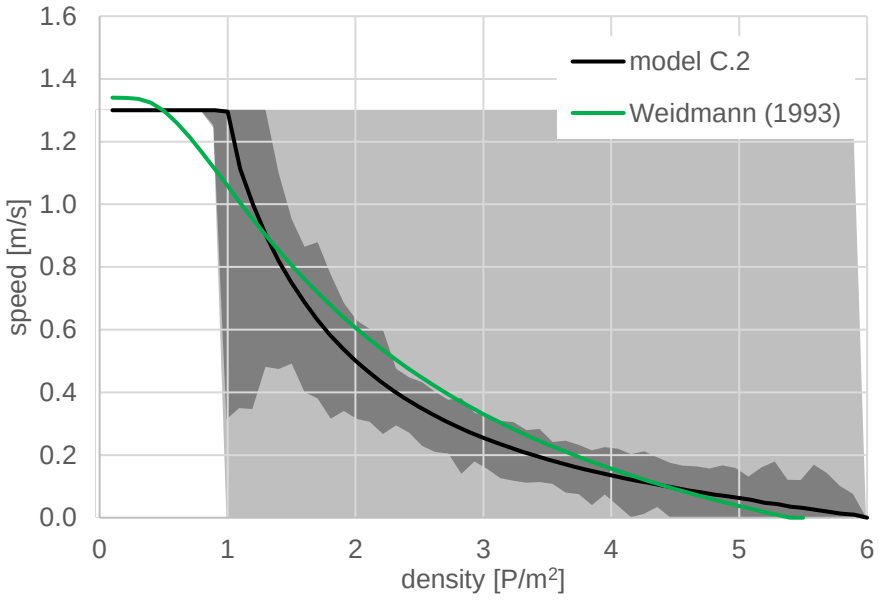

3.5.3 Step duration

For the calculation of the step duration, various formulas exist in literature. For comparison, and to study its effect, a different formula is used as well (Jelić et al., 2012).

$$D_s = \frac{0.065}{v} + 0.720 \quad (6)$$

D_s step duration [s]

v walking speed [m/s]

When comparing the fundamental diagram curves in Figure 11 and Figure 12, which have the same input data except the step length formula, only small differences are visible. Also, the range of instantaneous walking speeds is similar, only the average individual walking speed differ, but they are in a similar range.

Figure 12: Model C.3: Step duration calculated from Jelić et al. (2012).

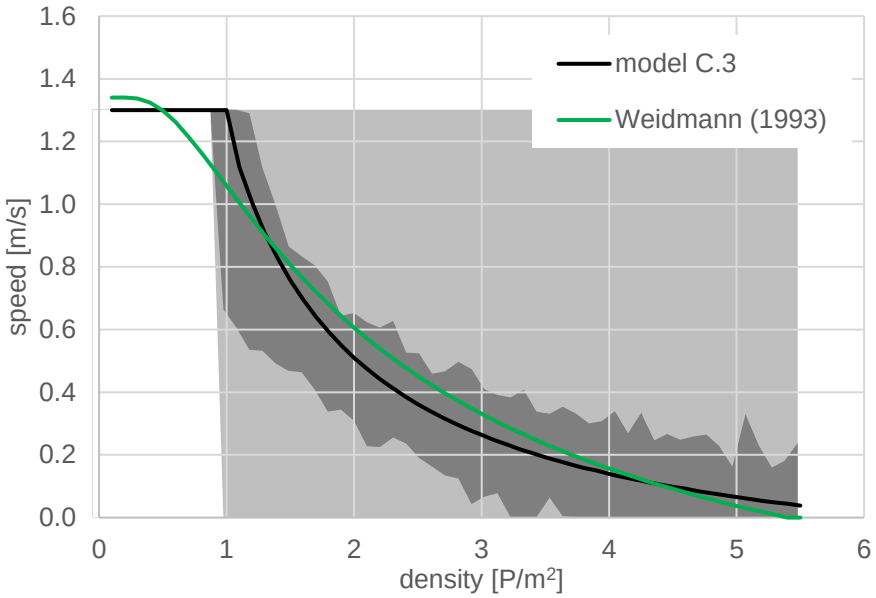

3.5.4 Acceleration limitation

Up until now, the model allows all speed changes to happen within one step, as no limit to the possible acceleration is set in the model. However, in reality maximum values exist which can be achieved due to physical constraints but also lower values can be found in literature which are based on comfort considerations of the pedestrians.

The previous model showed an unexpected stop and go behavior, which might occur due to strong acceleration and deceleration movements. Therefore, a maximum acceleration value of 0.6 m/s^2 is set. This value is relative low, but allows to see, if the limitation of the acceleration will influence the model results. But even when introducing the acceleration limitation, stop and go waves dominate the pedestrian flow in the model (Figure 13). Therefore, the maximum acceleration was further lowered to 0.3 m/s^2, but similar results were obtained (Figure 14). Compared to the previous model (Model C.4), the highest density, at which an average free flow speed occurs, is lower but at densities higher than about 2.4 P/m2, Model C.5 shows again

higher walking speeds. Nevertheless, the fundamental diagrams obtained are well within the range of expected values.

Figure 13: Model C.4: Fundamental diagram for a maximum acceleration of 0.6 m/s^2.

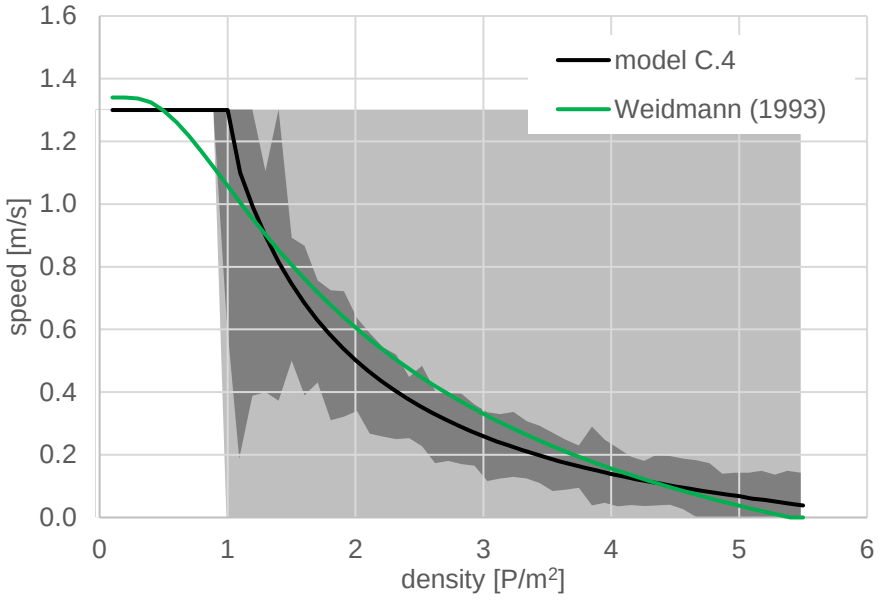

Figure 14: Model C.5: Fundamental diagram for a maximum acceleration of 0.3 m/s^2.

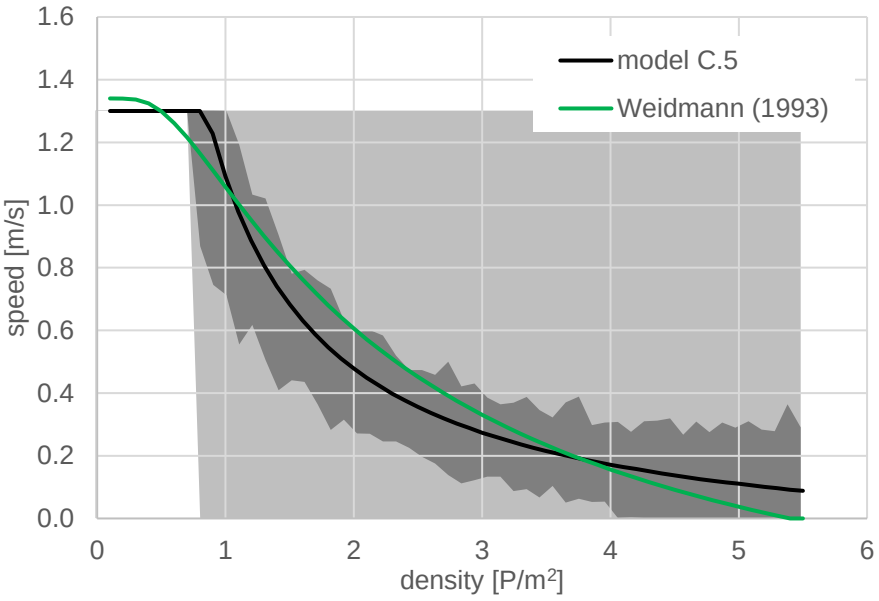

3.5.5 Random noise

Another model addition for the fundamental diagram based on lane movement, is the introduction of a random noise. The model does not include all aspects which are likely

determine to some extend the pedestrian walking characteristics, as well as an individual pedestrian does not react the same even in the same conditions. As first approach to also include these influences, a random noise is added to the model. The value for each speed update is calculated and a random noise, showing a standard distribution of 10% of the individual speed value, is added. This allows to study the effect of random variations on the fundamental diagram (Figure 15). In general, the average speed-density curve, as well as the speed distribution for a single time step, is similar to the previous model. Only at the free flow speed a speed distribution is visible, which did not occur previously.

Figure 15: Model C.6: Fundamental diagram with a random noise of 10%.

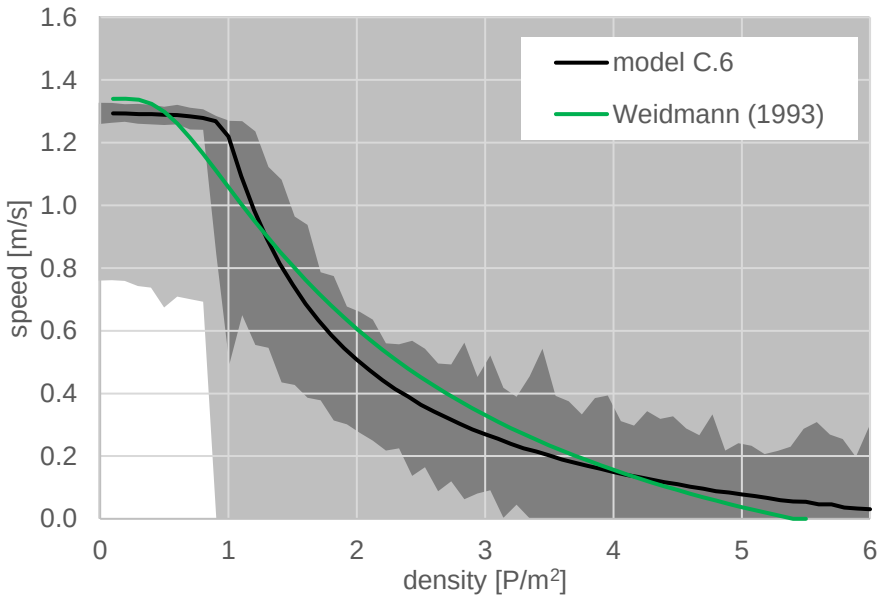

3.6 Model D: movement prediction

3.6.1 Introduction

As the human perception and the corresponding reaction takes some time, the movement decision is always based on outdated information. This is reflected in the previous model by introducing a reaction time, which separates the decision point from the action point. However, pedestrians, especially at steady state conditions, more or less move in a predictable manner. Thus, based on the information on its surrounding, a pedestrian can predict the movement of the other pedestrians and therefore adapt its walking behavior accordingly. To also reflect this

in the model, Model D introduces a movement prediction (Figure 16). At the decision point, the current speed is used to predict the position of the other pedestrian at the next action point, hence the beginning of the next step. This information is then used to determine the speed for the next step.

Figure 16: Modelled point of decision and action for a single step (Model D).

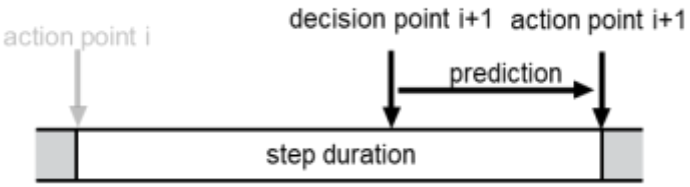

3.6.2 Model results

In Figure 17, the fundamental diagram for a uniform pedestrian distribution generated using Model D.2 can be seen. Compared to the previous model with the same parameter (Model C.6, Figure 15), lower average walking speeds at higher densities are visible. The curve of this model is again similar to the first models (Model A.2, Figure 3). The only visible difference is the small speed drop at densities lower than 1 P/m^2, which in Model A was always at the free-flow speed until the curve changed abruptly.

Figure 17: Model D.2: Fundamental diagram for a uniform pedestrian composition.

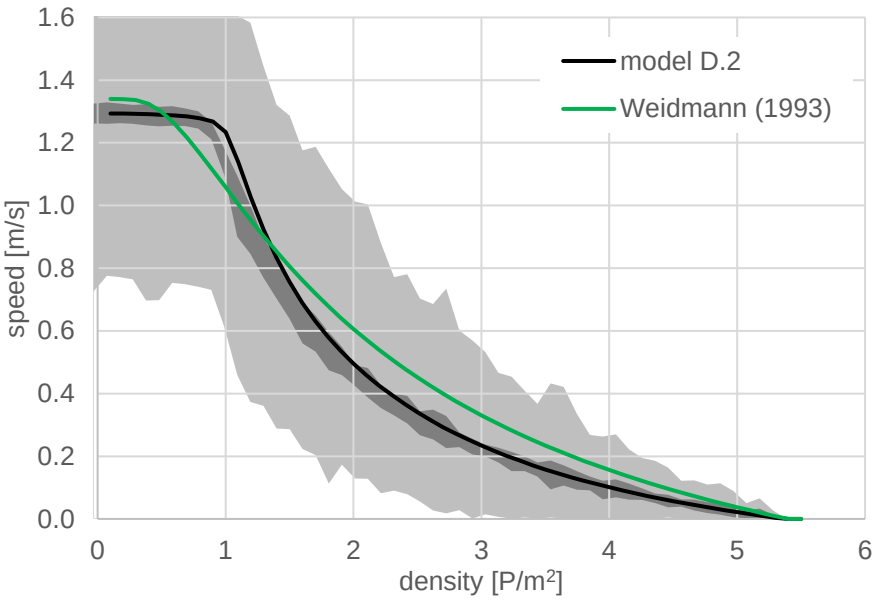

In the speed distribution shown in the graph stopping pedestrians only appear at densities higher than 3 P/m^2. Thus, stop-and-go waves are not present any more at low densities, as they were in the previous models. The distribution of average pedestrian speeds is only in a small range around the mean value. The instantaneous speed distribution gets narrower for higher walking speeds.

Figure 18: Model D.1, D.3, D.4: Fundamental diagrams with different pedestrian compositions (average, maximum, minimum). As a reference fundamental diagram from Weidmann (1993) and the speed-density data from literature compiled in Bosina and Weidmann (2017) are shown.

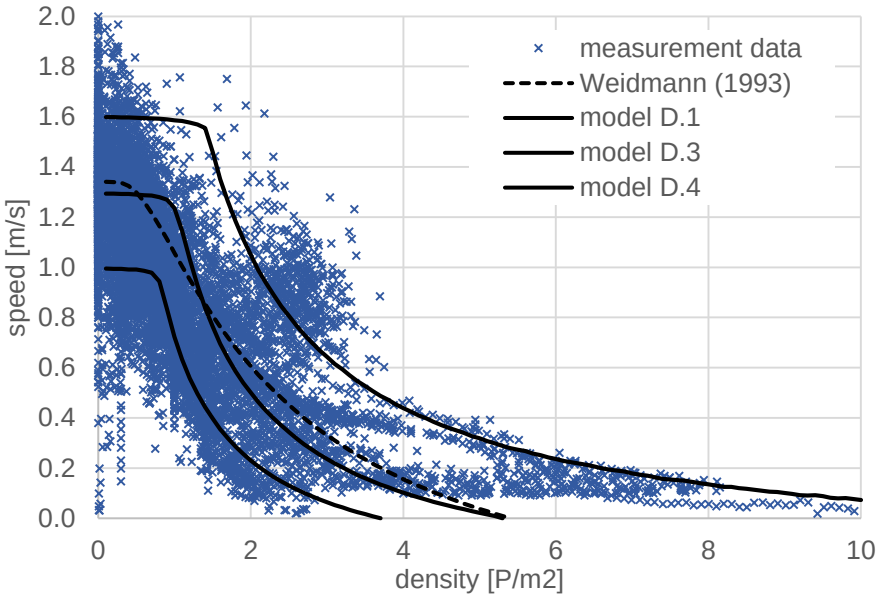

In Figure 18, the model simulations were done using the same model parameter as for Figure 17, but with different pedestrian populations. Similar to the results form Model A (Figure 3), the range of speed-density values is in the same range as the fundamental curves from the pedestrian populations using the minimum and maximum values. In comparison to the results from Model A, a visible difference only exists for the maximum distribution, where Model D.3 shows higher speed values at higher walking speeds and a higher maximum density. The reason for this can be seen in Figure 19, where also the speed distribution is computed. In contrast to the other simulations using Model D, stop-and-go waves are visible. Here, also the average pedestrian speeds are widely distributed.

Still, a direct comparison between the calculated fundamental diagrams and the speed-density values from literature has to be made with caution. First, the speed density values are often

disaggregated values, whereas the model results are the mean from all pedestrians in steady state conditions. Second, the model is still based on a lane-movement approach.

Figure 19: Model D.3: Fundamental diagram for a maximum pedestrian composition.

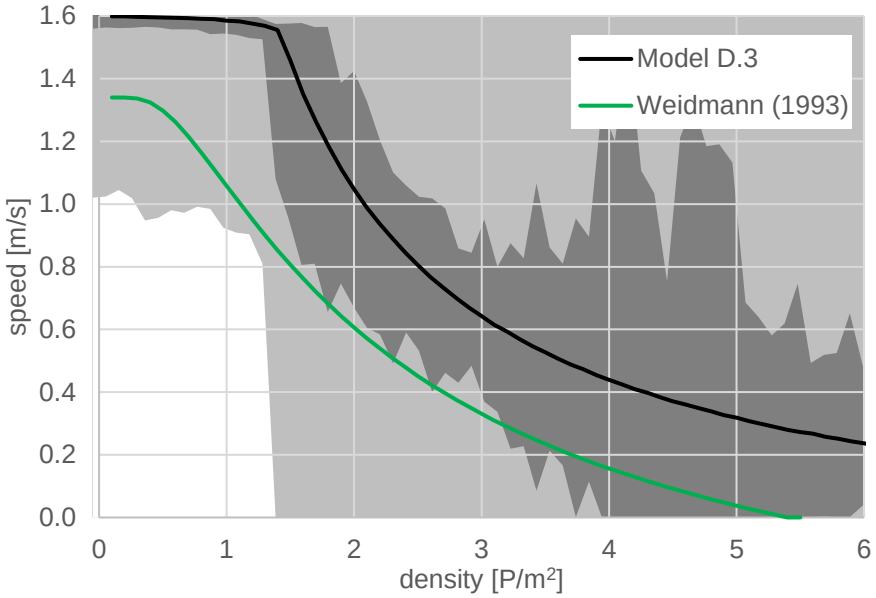

3.6.3 Free-flow speed

Figure 20: Model D.2 and D.5: Fundamental diagrams for a uniform pedestrian composition with an average (Model D.2) and a uniform (Model D.5) desired walking speed distribution.

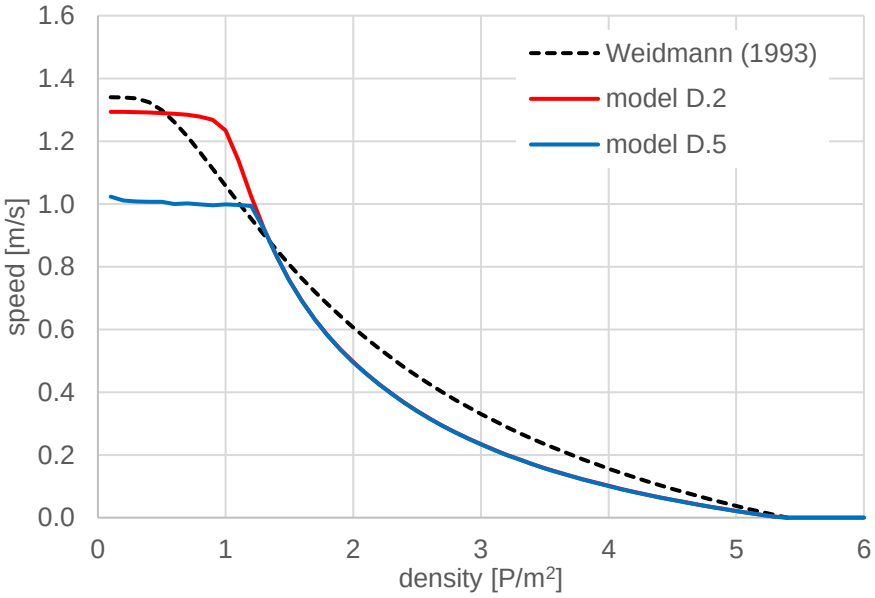

Up until now, the uniform distribution uses only the average free-flow walking speed, as otherwise the fundamental diagrams calculated would be only determined by the slowest person. To visualize the effect of the distribution of the free-flow speed, Figure 20 compares the fundamental diagrams obtained from Model D.2 and Model D.5. Whereas in Model D.2, an average free-flow walking speed is used for all pedestrians, a uniform speed distribution exists in Model D.5. As expected, these two models are only different at densities lower than 1.2 P/m^2, where the average walking speed is higher than 1.0 m/s in Model D.2.

3.7 Model Comparison

To compare all lane-based fundamental diagram models presented, Figure 21 shows a comparison of the results from the different models until now. For each model, a simulation was selected having the same parameter values. The comparison shows that the model results are quite similar for all models, hence the model extensions made did not change the results strongly. Nevertheless, the results from last model (Model D.2) do show certain improvements. The transition from the free-flow phase to the restricted phase at about 1.0 P/m^2 is not as abrupt as in the first models. In addition, for most parameter values, stop-and-go waves are only visible at high walking speeds, which corresponds to the microscopic behavior also visible in real-life situations.

To extend the linear model to a speed-density model and therefore to allow the calculation of two dimensional fundamental diagrams, a lane width was calculated. Therefore, by running the model only for single lanes, the speed-density relation for single-file movement can be calculated.

The first comparison with literature data and the fundamental diagram from Weidmann (1993) shows that the range of fundamental diagrams obtained from the model correspond to the expected range. To validate this model, it must be compared to data from lane movement experiments. In addition, the model results can be compared to unidirectional fundamental diagrams to see, if this model is already able to reproduce the difference observed also in this case.

Figure 21: Model A.2, B.1, C.6, D.2: Comparison of the fundamental diagram curves for the different lane-based models and the fundamental diagram proposed by Weidmann (1993).

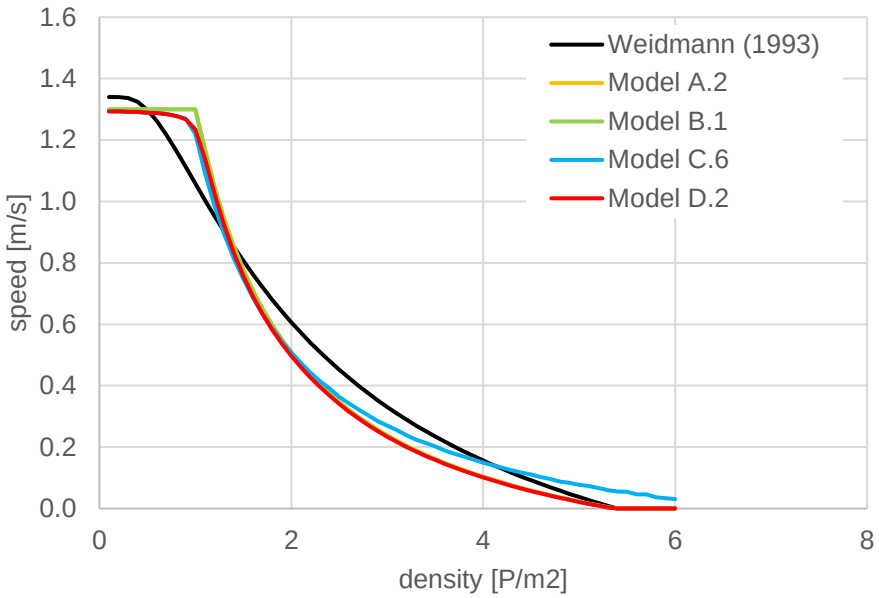

4. Lane-change model

4.1 Model description

Although the results of the lane-based models are within the range of expected values, they are not capable of adequately describe the influence of the free-flow speed distribution, as overtaking is not possible. To tackle this problem, a model extension is made, which allows the pedestrians to change from one lane to a neighboring one. The pedestrians are still walking in lanes, but, if enough space is available, swapping lanes is possible. This allows to walk past slower pedestrians. As no side preference as well as walking on a specific side is implemented, the pedestrians will stay in the new lane until a further lane change is made.

4.2 Model layout

To integrate the lane-change behavior into the existing model, a simple lane-changing model will be established. For this, several lanes as they are modelled in Model D will be run simultaneously. At each time step, a routine will be introduced, which will first determine, if a pedestrian wants to change the lane and then move the pedestrian from one lane to the other.

The decision, if a pedestrian in changing a lane is considered to be based on the current walking speed and the headway. If the current walking speed is lower than the desired walking speed and the headway is smaller than the same position in a neighboring lane, a lane change is desired. In addition, a backward free space is set for the neighboring lane to avoid conflicts with other pedestrians. Another threshold value is set for the maximum headway to the pedestrian in front. If the headway is higher than this value, no lane change is made, as enough space is available to increase the speed.

The lanes are again aligned in a circle; hence all lanes have two equal neighbors. If both neighboring lanes fulfil the requirements for a lane change, the one providing a longer headway is used for changing to.

A pedestrian can change the lane at the beginning of each step. As the model is kept simple, the lane change decision is based on the current distances at this time and is done immediately. In reality it would be expected that also the decision on the lane change is done beforehand and that the lane-change procedure needs some time in which both lanes are blocked to some extent.

On the other hand, the walking speed is not updated when changing lanes, hence the walking speed calculated from the lower previous headway is used.

The initial positioning of the pedestrians and the initial speed is set randomly, hence also bigger gaps can occur. To avoid lane changes based on the initial conditions, lane-changing is only allowed after a defined number of time steps. Otherwise it might be possible, that pedestrians move to another lane due to the initial conditions and then cannot move away any more when the initial gaps are closed.

To study the effect of different parameter settings on the simulation results, several simulation runs were made (Table 6). First, different pedestrian distributions were simulated. Then, the minimal distance to pedestrians in the back was varied, to see the influences on the results.

Table 6: Parameter values used in this chapter.

Model	Pedes-trians	Duration [s]	Distribution	Back distance [m]	Steps without lane change	Max. Head-way [m]	Figure
E.1	100	1000	average	3	100	4	Figure 25
E.2	100	1000	uniform	3	100	4	Figure 22 Figure 24
E.3	100	1000	maximum	3	100	4	Figure 25
E.4	100	1000	minimum	3	100	4	Figure 25
E.5	100	1000	uniform	3	100	4	Figure 23 Figure 24
E.6	100	1000	uniform	2	100	4	Figure 24
E.7	100	1000	uniform	1	100	4	Figure 24
E.8	100	1000	uniform	0.5	100	4	Figure 24

4.3 Model E: results

For simulations without variations in the free-flow speed, the results are similar to the ones obtained using Model D. In Figure 22 the resulting fundamental diagram and speed distribution from Model E.2 can be seen. In comparison to the results from Model D.2 (Figure 17), where the same parameter values were used, only a slight increase in the speed variations is visible. This also corresponds to the expectations. At low densities, where free-flow speed is simulated, no need to overtake is present, as everyone has the same free-flow walking speed. At high walking speeds, no big enough gaps exist which will make a lane-change possible in the model. In addition, the distribution of the other parameters seems not to be big enough to trigger lane-change behavior also at medium densities.

Figure 22: Model E.2: Fundamental diagram for a uniform pedestrian composition without variations in the desired walking speed.

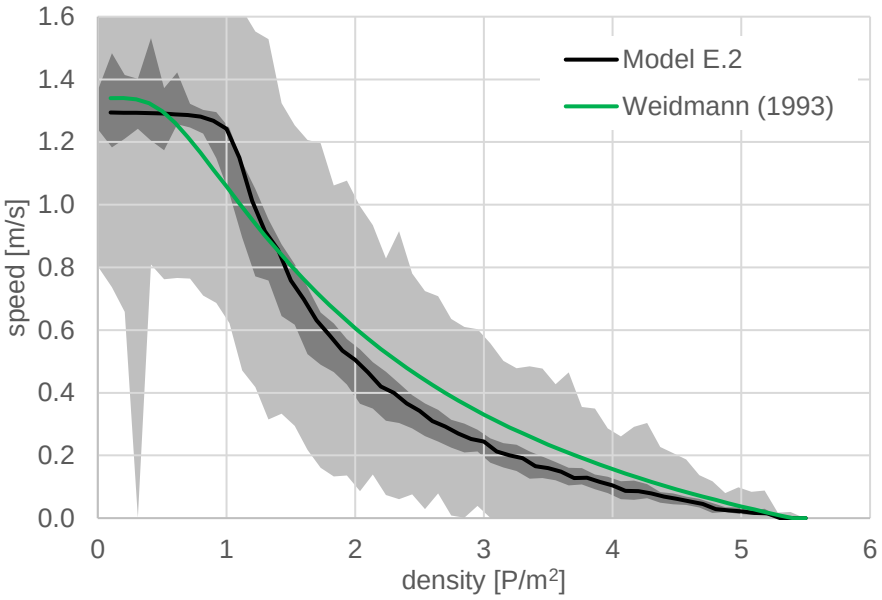

In the previous model, a distribution of free-flow speeds lead to an average walking speed of the minimum free-flow speed at low densities. As can be seen in Figure 23, the possibility to change lanes allows to walk past slower pedestrians, which leads to higher walking speeds in this density region. Still, the walking speed is not as high as the walking speed for Model E.2, which has an average free-flow walking speed for all pedestrians. For higher densities, the two fundamental diagram curves do not show any differences. The free-flow speed distribution can also be seen in the walking speed distribution, where a higher range can be seed for a distributed free-flow speed.

The possibility to overtake is strongly determined by the parameter which determines the minimal backwards distance to be allowed to change to another lane. The bigger the value is, the more space is needed for the lane-change, hence the less overtaking occurs. Otherwise, if the minimal backwards distance is reduced, it becomes more likely for pedestrians from the back to be forced to slow down as they will otherwise collide with the pedestrian who changed from one lane to another. The resulting fundamental diagrams from simulations with different parameter values are visible in Figure 24. A slight increase in the mean walking speed for shorter minimal backward distances can be seen, but the differences are small.

Figure 23: Model E.5: Fundamental diagrams for a uniform pedestrian composition with a uniform desired walking speed distribution.

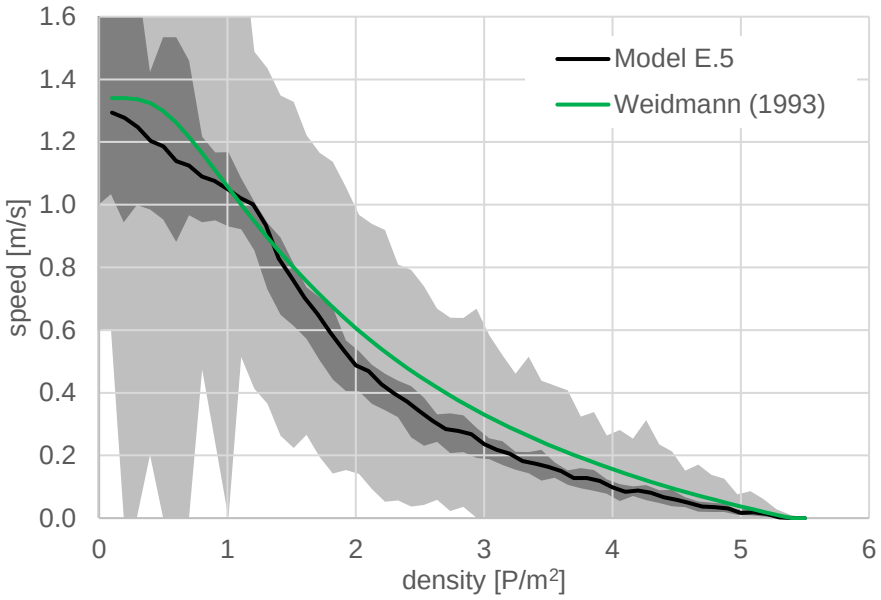

Figure 24: Model E.2 and Model E.5 to E.8: Influence of different minimum backward distance for lane change on the fundamental diagram. For comparison, Model E.2 shows the results for a single free-flow speed for all pedestrians

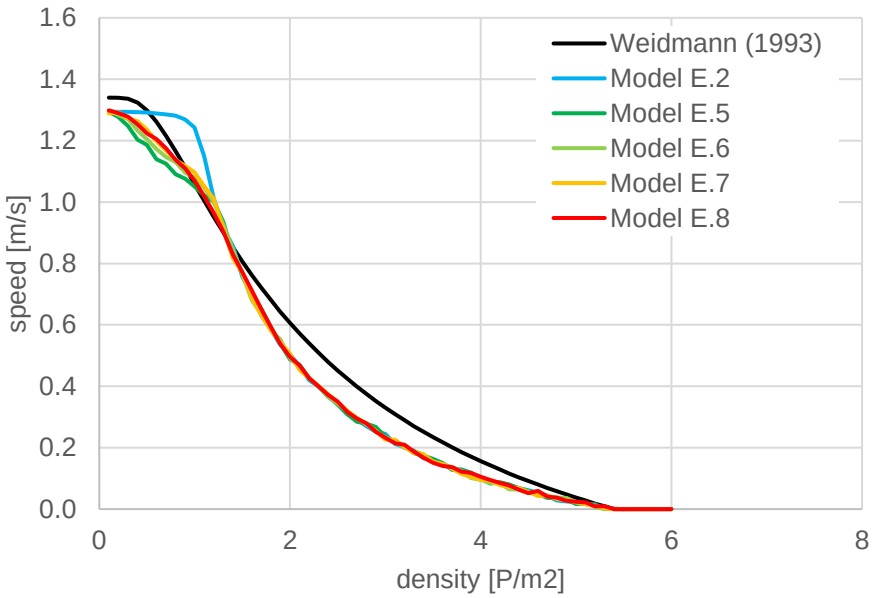

The first model results for Model E show that the model is able to include the overtaking procedure in the fundamental diagram calculations by establishing a lane change procedure. The model results suggest that distributed free-flow speed values lead to slower walking speeds compared to a single free-flow speed for all pedestrians at otherwise the same parameter values.

5. Conclusion

Both, the lane-change and lane-based models were already able to reproduce fundamental diagrams close to the expected values. Both are expected to be sufficient for providing a situation specific fundamental diagram useful for the design of pedestrian facilities. As the lane-change model (Model E) is also able to simulate overtaking behavior and therefore study the effect of different free-flow speed distributions, this model will be selected for the further modelling steps. Nevertheless, the lane-based models all result in similar fundamental diagram curves. Therefore, if simulation time is an issue, it might be useful to test if this model is also able to fulfil the requirements.

Figure 25: Model E.1, E.3, E.4: Fundamental diagrams with different pedestrian compositions (average, maximum, minimum). As a reference fundamental diagram from Weidmann (1993) and the speed-density data from literature compiled in Bosina and Weidmann (2017b) are shown.

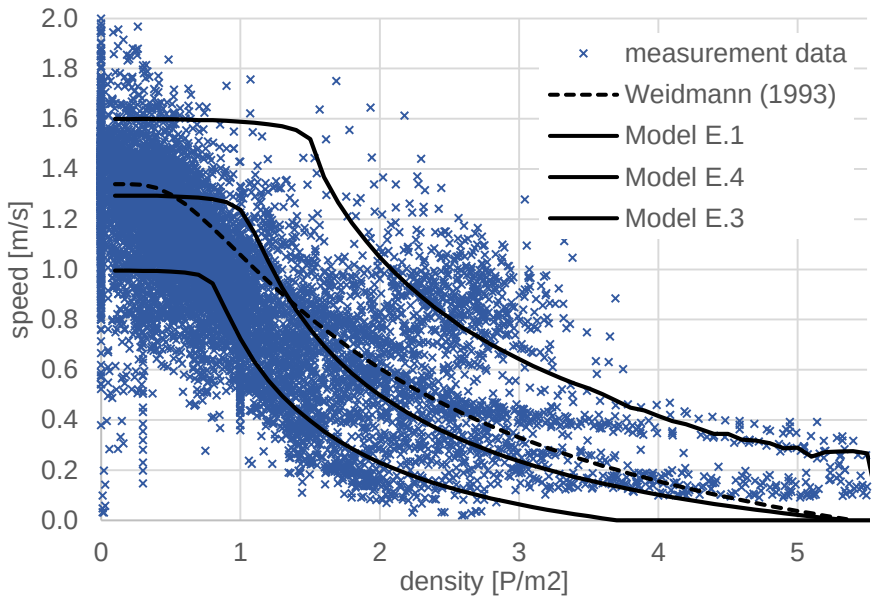

Figure 25 shows the fundamental diagram curves for different pedestrian compositions to estimate the resulting range of Model E. Therefore, in a next step, the model will be calibrated, verified and validated to determine the quality of the model. The preliminary conclusion can be made that it seems to be possible to reproduce the shape of the fundamental diagram already with simple generic models. The stepwise approach was found to be useful, as it was possible to determine the influence of each gain in complexity and therefore obtain a good understanding of the model behavior.

6. References

Bosina, E. and U. Weidmann (2017) Estimating pedestrian speed using aggregated literature data, *Physica A: Statistical Mechanics and its Applications*, **468** 1–29.

Bosina, E. and U. Weidmann (2016) Generic Description of the Pedestrian Fundamental Diagram, W. Song, J. Ma and L. Fu (eds.), in *Proceeding of Pedestrian and Evacuation Dynamics 2016*, University of Science and Technology of China Press, paper presented at *Pedestrian and Evacuation Dynamics PED 2016*, Hefei, China, 2016.

Cao, S., J. Zhang, D. Salden, J. Ma, C. Shi and R. Zhang (2016) Pedestrian dynamics in single-file movement of crowd with different age compositions, *Physical Review E*, **94** (1) 012312.

Cavagna, G.A. and R. Margaria (1966) Mechanics of walking, *Journal of Applied Physiology*, **21** (1) 271–278.

Degond, P., J. Pettré, S. Donikian, C. Appert-Rolland, A. Jelić, S. Lemercier, J. Hua, J. Narski and J. Fehrenbach (2015) Time-delayed follow-the-leader model for pedestrians walking in line, *Networks and Heterogeneous Media*, **10** (3) 579–608.

DIN Deutsches Institut für Normung (2013) Wesentliche Maße des menschlichen Körpers für die technische Gestaltung - Teil 2: Anthropometrische Datenbanken einzelner nationaler Bevölkerungen, *DIN CEN ISO/TR 7250-2, DIN SPEC 91279*.

Duives, D.C., W. Daamen and S.P. Hoogendoorn (2013) State-of-the-art crowd motion simulation models, *Transportation Research Part C: Emerging Technologies*, **37** 193–209.

Guy, S.J., J. Chhugani, S. Curtis, P. Dubey, M. Lin and D. Manocha (2010) PLEdestrians: A Least-effort Approach to Crowd Simulation, in *Proceedings of the 2010 ACM SIGGRAPH/Eurographics Symposium on Computer Animation*, *SCA '10*, Eurographics Association, Aire-la-Ville, Switzerland, Switzerland, 2010.

Hall, E.T. (1966) *The Hidden Dimension*, Doubleday, New York.

Hediyeh, H., T. Sayed and M.H. Zaki (2015) The use of gait parameters to evaluate pedestrian behavior at scramble phase signalized intersections, *Journal of Advanced Transportation*, **49** (4) 523–534.

Helbing, D. and P. Molnár (1995) Social force model for pedestrian dynamics, *Physical Review E*, **51** (5) 4282–4286.

Jelić, A., C. Appert-Rolland, S. Lemercier and J. Pettré (2012) Properties of pedestrians walking in line. II. Stepping behavior, *Physical Review E*, **86** (4) 1–8.

Kang, W. and Y. Han (2017) A Simple and Realistic Pedestrian Model for Crowd Simulation and Application, *arXiv:1708.03080 [nlin]*, arXiv: 1708.03080.

Kramers-de Quervain, I.A., E. Stüssi and A. Stacoff (2008) Ganganalyse beim Gehen und Laufen, *Schweizerische Zeitschrift für «Sportmedizin und Sporttraumatologie*, **56** (2) 35–42.

Ma, J., W. Song, Z. Fang, S. Lo and G. Liao (2010) Experimental study on microscopic moving characteristics of pedestrians in built corridor based on digital image processing, *Building and Environment*, **45** (10) 2160–2169.

Moussaïd, M., D. Helbing, S. Garnier, A. Johansson, M. Combe and G. Theraulaz (2009) Experimental study of the behavioural mechanisms underlying self-organization in human crowds, *Proceedings of the Royal Society B: Biological Sciences*, **276** (1668) 2755–2762.

Moussaïd, M., D. Helbing and G. Theraulaz (2011) How simple rules determine pedestrian behavior and crowd disasters, *Proceedings of the National Academy of Sciences*, **108** (17) 6884–6888.

Murray, M.P., A.B. Drought and R.C. Kory (1964) Walking Patterns of Normal Men, *The Journal of Bone and Joint Surgery. American Volume*, **46** (2) 335–360.

Pheasant, S. (2006) *Bodyspace: anthropometry, ergonomics, and the design of work*, Taylor & Francis, Boca raton.

Portz, A. and A. Seyfried (2011) Analyzing Stop-and-Go Waves by Experiment and Modeling, in R. D. Peacock, E. D. Kuligowski and J. D. Averill (eds.), *Pedestrian and Evacuation Dynamics*, 577–586, Springer US.

Reda, F.A. (2017) *Crowd motion modelisation under some constraints*, dissertation, Université Paris-Saclay, Paris.

Seitz, M.J. and G. Köster (2012) Natural discretization of pedestrian movement in continuous space, *Physical Review E*, **86** (4) 046108.

Simoneau, G.G. (2010) Kinesiology of Walking, in *Kinesiology of the Musculoskeletal System: Foundations for Rehabilitation*, 627–681, Mosby, St. Louis, Mo.

Still, K. (2000) *Crowd Dynamics*, dissertation, University of Warwick, Warwick.

Weidmann, U. (1993) *Transporttechnik der Fussgänger - Transporttechnische Eigenschaften des Fussgängerverkehrs (Literaturauswertung)*, Institut für Verkehrsplanung, Transporttechnik, Strassen- und Eisenbahnbau, ETH Zürich, Zürich.

Zhang, J., S. Cao, D. Salden and J. Ma (2016) Homogeneity and Activeness of Crowd on Aged Pedestrian Dynamics, *Procedia Computer Science*, **83** 361–368.

Ziemer, V., A. Seyfried and A. Schadschneider (2016) Congestion Dynamics in Pedestrian Single-File Motion, in *Traffic and Granular Flow '15*, 89–96, Springer, Cham.